Biochimica et Biophysica Acta, 765 (1984) 74–83
Elsevier

BBA 41471

BINDING AND RELEASE KINETICS OF INHIBITORS OF Q_A^- OXIDATION IN THYLAKOID MEMBRANES

WIM F.J. VERMAAS, GERHARD DOHNT AND GERNOT RENGER *

Max-Volmer-Institut für Biophysikalische und Physikalische Chemie, Technische Universität Berlin, Sekr. PC 14, Strasse des 17. Juni 135, D-1000 Berlin-12 (Germany)

(Received November 28th, 1983)

Key words: Photosystem II; Herbicide; Plastoquinone; Oxygen evolution

Oxygen flash yield patterns of dark adapted thylakoid membranes as measured with a Joliot-type O_2-electrode indicate that inhibitors that block the oxidation of the reduced primary quinone Q_A^- of Photosystem II vary greatly in the rate of binding to and release from the inhibitor/Q_B binding environment. The 'classical' Photosystem-II herbicides like diuron and atrazine exhibit slow binding and release kinetics, whereas, for example, phenolic inhibitors, *o*-phenanthroline and synthetic quinones are exchanging quite rapidly with Q_B (about once per second or faster at inhibitor concentrations causing about 50% inhibition of O_2 evolution). No general relationship between the efficiency of the inhibitor and the exchange rate is observed; it depends mainly on the type of inhibitor. Based on the classical Kok model, equations are derived in order to calculate oxygen yields evolved by thylakoids in single-turnover flashes as a function of the rate constants of inhibitor binding to and release from the inhibitor/Q_B binding environment in the presence of an oxidized or semireduced $Q_A \cdot Q_B$ or $Q_A \cdot$ inhibitor complex. Fitting of theoretical and experimental values yields that *o*-phenanthroline binds much faster to an oxidized than to a semireduced $Q_A \cdot Q_B$ complex. This fits very well with the hypothesis that the Q_B^- affinity to the site is much higher than that of Q_B. In the case of *i*-dinoseb, however, inhibitor/quinone exchange seems to occur mainly in the semiquinone state. Possibilities to explain this result are discussed.

Introduction

Inhibitors from many different classes are known to block the oxidation of the reduced primary electron accepting quinone, Q_A^-, by the secondary quinone, Q_B [1,2]. Almost without exception the inhibitors bind to such a region in the proteinaceous inhibitor/quinone binding environment that the affinity for binding of many other inhibitors and of the native plastoquinone (Q_B) is decreased by orders of magnitude or is completely abolished ('competitive binding' of inhibitors and quinones) [3–5]. Although for many inhibitors the dissociation constant has been determined [6–8], only a few results on the kinetic constants of binding and release have been reported [9–11].

The affinity of plastoquinone for the Q_B binding site is probably rather low in the fully oxidized and fully reduced state; in the semiquinone form, Q_B^-, however, the affinity is assumed to be high [5]. This explains the high stability of Q_B^- in the dark. The DCMU binding is altered upon a change in the Q_B^- concentration [12] in a way best explica-

* To whom reprint requests should be addressed.

Abbreviations: DCMU, 3-(3′,4′-dichlorophenyl)-1,1-dimethylurea; DNOC, 4,6-dinitro-*o*-cresol; Q_A, primary electron-accepting quinone in Photosystem II; Q_B, secondary electron-accepting quinone in Photosystem II; Inh, inhibitor; DCIP, 2,6-dichlorophenolindophenol; Tricine, *N*-[2-hydroxy,-1,1-bis(hydroxymethyl)ethyl]glycine.

ble by assuming a low DCMU-affinity in those chains that have a semireduced quinone acceptor complex ($(Q_A \cdot Q_B)^-$) and a high DCMU affinity in chains with an oxidized $Q_A \cdot Q_B$ complex. This is in good agreement with the hypothesis that the Q_B affinity is dependent on the redox state of the quinone complex.

In this study, a new approach is used for measuring inhibitor and plastoquinone binding to and release from the inhibitor/Q_B binding environment as a function of the redox state of the quinone complex: inhibitor/Q_B exchange is probed by the O_2 evolution as a function of flash number as measured with a Joliot-type O_2 electrode. It is well-known that O_2 evolution of previously dark-adapted thylakoids induced by single-turnover flashes oscillates with a period of 4 [13]. The O_2 evolution oscillations can be described quite well by the model of five S-states (S_0–S_4) as proposed by Kok et al. [14]. 'Misses' and 'double-hits' (with probability α and β, respectively) induce the damping of the oscillation. Since most (if not all; see Ref. 15) of the reaction chains are in state S_1 after thorough dark adaptation, the maximum O_2 evolution occurs at the third flash.

When considering the flash-induced O_2-evolution in previously dark-adapted thylakoids in the presence of moderate concentrations of Q_A^- oxidation inhibitors (inhibiting 20–80% of the O_2 evolution), there are two possibilities for the shape of the flash pattern.

(1) Within the time of the flash train no displacement of the inhibitor by Q_B or vice versa occurs. This implies that the reaction chains that have not bound an inhibitor molecule will behave like the control, whereas the other chains will not make more than one net turnover (producing no O_2). Such a 'static' situation results in an oscillation pattern with normal damping but with a decreased amplitude.

(2) Within the time of the flash train the inhibitor molecule has a high probability to be displaced by Q_B and vice versa. After an inhibitor molecule (that was already bound to the site before the first flash) is replaced by Q_B during the flash train, the reaction chain will start out in state ($S_1 \cdot Q_A \cdot Q_B$) or ($S_2 \cdot Q_A \cdot Q_B^-$), irrespective of the number of flashes fired before the inhibitor molecule was released. This reaction chain may be 'out of phase' with the 'permanently uninhibited' chains. On the other hand, reaction chains in which Q_B is replaced by an inhibitor molecule will not make more than one net turnover and will remain mainly in the ($S_n \cdot Q_A^- \cdot$ Inh) state (Inh means inhibitor) until the inhibitor molecule is replaced by Q_B again. Such center may also be 'out of phase' with the uninhibited center when they bind Q_B. It is clear that such a dynamic inhibitor-Q_B interaction does not only lead to an inhibited O_2 evolution, but also to an increased damping of the oscillation.

If the residence time of the inhibitor at the binding environment is of the same order of magnitude as the duration of the flash train, rather large differences in flash pattern are expected when comparing a flash pattern obtained at high frequency with one obtained at a lower frequency. In the former case, the inhibitor molecule will exchange less than in the latter case, resulting in an increase of damping at decreasing flash frequency.

Based on these considerations, calculations have been made in order to estimate the binding and release kinetics of inhibitors as a function of the redox state of the quinone complex.

A preliminary report on this subject has been presented at the 6th International Congress on Photosynthesis in Brussels (August 1–6, 1983).

Materials and Methods

The thylakoid isolation from pea leaves as well as measurements using an unmodulated Joliot-type O_2-electrode have been described in Ref. 15. After isolation, the thylakoids were suspended in the reaction medium at pH 7.6, consisting of 50 mM Tricine-NaOH/10 mM NaCl/5 mM $MgCl_2$/0.3 M sorbitol (see Ref. 15). When a certain concentration of inhibitor was to be added, the thylakoids were washed once at low chlorophyll concentration (10 $\mu g \cdot ml^{-1}$) with this inhibitor concentration before resuspension to 0.8 $mg \cdot ml^{-1}$ chlorophyll in a medium with the inhibitor. In this way the added inhibitor concentration can be kept approximately equal to the free inhibitor concentration after binding equilibration in the dark.

The thylakoids were kept in the dark on ice, and were transferred to the Pt-electrode surface of

the Joliot electrode in very dim light. No significant turnover of Photosystem II (as measured by a change in the flash pattern observed 0.5 min after transfer compared to that observed 5 min after transfer) was detectable upon transfer. The thylakoids were dark adapted additionally for 5 min and the O_2 evolution pattern at 4, 2, 1 or 0.5 Hz flash frequency was measured.

Results and Discussion

Qualitative estimation of inhibitor / Q_B exchange

As outlined above, it can be determined qualitatively whether Q_B-inhibitor exchange occurs in the time between flashes by measuring the O_2 yield oscillation as a function of flash number in the presence of the inhibitor. Using inhibitor concentrations that blocked O_2 production by approx. 50%, large differences in O_2 evolution pattern were observed for different inhibitor groups. The 'classical' Photosystem II herbicides (DCMU, atrazine) do not damp the O_2 evolution pattern (Fig. 1 and Table I), whereas many others (*i*-dinoseb, *o*-phenanthroline, quinone-type inhibitors) increase the damping (Table I), especially at lower flash frequency (Fig. 1). This indicates that, in the case of *i*-dinoseb, there is a significant inhibitor/Q_B exchange when the time between the flashes is 2 s, but that the exchange is much less at a 4 Hz flash frequency. Therefore, the rate of exchange in the presence of 1 μM *i*-dinoseb seems to be in the

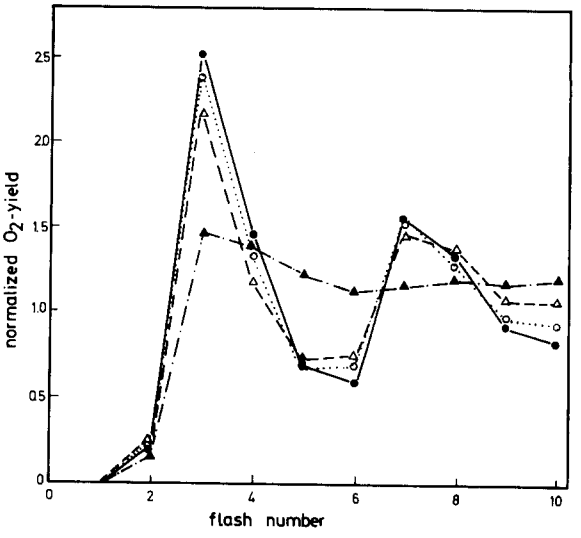

Fig. 1. Single-turnover flash-induced oxygen evolution pattern of previously dark-adapted pea thylakoids as a function of flash number. The flash frequency was 0.5 Hz. ●, control; ○, +0.1 μM atrazine; ▲, +1 μM *i*-dinoseb; △, +1 μM *i*-dinoseb, but at 4 Hz flash frequency. The chlorophyll concentration was 0.8 mg·ml^{-1}. The oxygen flash yields were normalized to an average of 1.0 over the ten flashes. The concentration of inhibitors used inhibited the O_2 evolution by 60–70%.

TABLE I

RATES OF Q_B/INHIBITOR EXCHANGE

Qualitative rates of inhibitor-Q_B exchange at the common binding environment near Q_A in pea thylakoids as measured with a Joliot-type O_2-electrode. In this table, the exchange rates are defined as 'fast' when, at flash frequencies of 1 Hz or more, considerably more damping of the O_2 yield oscillation occurs than in the control; in this case, the exchange rates are in the order of 0.1–1 s^{-1} or more. The inhibitor was added in such a concentration that the O_2 evolution was inhibited by about 50%.

Inhibitor	Class	Approx. pI_{50}	Damping of oscillation	Inhibitor/Q_B exchange rate
DCMU	urea	7.5	−	slow
Atrazine	s-triazine	7.0	−	slow
Phenisopham	biscarbamate	6.8	−	slow
i-Dinoseb	nitrophenol	5.9	+	fast
4,6-Dinitro-*o*-cresol	nitrophenol	4.8	+	fast
Bromoxynil	nitrile	6.0	−	slow
Metamitron	triazinone	6.0	+ −	intermediate
o-Phenanthroline	−	5.8	+	fast
Tetrachloro-*p*-benzo-hydroquinone	quinone	4.8	+	fast
2-Hydroxy-3-(11-oxododecyl)-1,4-naphthoquinone	quinone	6–7	+	fast

order of 0.5 s^{-1}. There is not a good relationship between the pI_{50} of the inhibitor and the exchange rate (Table I). The inhibitor binding and the release kinetics appear to be governed primarily by the structure of the inhibitor. It is striking that bromoxynil – and also ioxynil (data not shown) – does not behave like the other phenolic inhibitors (DNOC and *i*-dinoseb), supporting the idea that bromoxynil and ioxynil do not belong to the group of the phenolic herbicides but rather to a separate group, that of the 'nitriles'. The quinone-type inhibitors are exchanging quite rapidly with Q_B, supporting the hypothesis of a rapid binding and release of the analogous quinone Q_B.

A relatively slow binding and release of certain inhibitors may suggest a high activation energy between the free and bound state of that inhibitor. Further experiments and considerations are needed in order to clarify the reason for a large difference in activation energy for binding and release between certain groups of inhibitors. For such considerations also the possibility of the existence of more than one inhibitor-binding environment has to be taken into account, in which inhibitor binding to one environment changes the other environments such that the bindings affinity of inhibitors binding to those domains is greatly diminished. Such a mechanism may provide a good explanation for the observation that [^{14}C]ioxynil and [^{14}C]atrazine binding is not completely abolished after covalent linkage of an azidoquinone to the inhibitor/Q_B binding environment [3].

Quantitative calculation of exchange parameters

In the Appendix, equations are derived from which the theoretical O_2-evolution oscillation patterns as a function of the exchange parameters E_n ($1 \leqq n \leqq 4$) as defined below in reactions 1 and 2 can be calculated. The theoretical patterns are compared to the experimental ones, and the best fitting set of exchange parameters is selected. The calculations and/or the theoretical O_2 patterns derived thereof are based on the following assumptions:

(a) The classical Kok model [14], in which the α and β parameters do not depend on the S-states, can also in this case describe the O_2 evolution as a function of flash number. However, some extensions of the model are required: in state ($S_n \cdot Q_A \cdot Q_B$) and ($S_n \cdot (Q_A \cdot Q_B)^-$) α and β are unchanged compared to the control; in state ($S_n \cdot Q_A \cdot$ Inh) $\beta = 0$ and α is unchanged, and in state ($S_n \cdot Q_A^- \cdot$ Inh) $\alpha = 1$ and $\beta = 0$.

(b) After thorough dark adaptation all reaction chains are in state ($S_1 \cdot Q_A \cdot Q_B$) or ($S_1 \cdot Q_A \cdot$ Inh). S_0 is assumed not to be present [15], and the Q_B^-/Q_B ratio in the presence of inhibitors was found to be less than 1/15 in our conditions (as measured by DCMU-induced fluorescence in the presence of NH_2OH).

(c) Between the flashes the following reactions occur:

$$S_n \cdot Q_A \cdot Q_B + \text{Inh} \underset{E_1}{\overset{E_3}{\leftrightarrows}} S_n \cdot Q_A \cdot \text{Inh} + PQ \quad (1)$$

$$S_n \cdot (Q_A \cdot Q_B)^- + \text{Inh} \underset{E_2}{\overset{E_4}{\leftrightarrows}} S_n \cdot Q_A^- \cdot \text{Inh} + PQ \quad (2)$$

$$S_n \cdot Q_A^- \cdot \text{Inh} \xrightarrow{k} S_{n-1} \cdot Q_A \cdot \text{Inh} \quad (3)$$

In reactions 1 and 2, $0 \leqq n \leqq 3$; for reaction 3, $n = 2$ or 3. It is assumed here that a back reaction between Q_A^- and S_3 can occur; it is not clear at this moment whether this assumption is correct; however, the maximal $S_3 \cdot Q_A^-$ fraction is low, since it can only be formed in the reaction chains that are connected to a one-electron donor (see assumption (b)), which is able to reduce S_2 or S_3 only once with a half-time of 1.4 s [15]. After dark adaptation in our conditions only about 20% of the reaction chains have this donor [15]. The back reaction of $(Q_A \cdot Q_B)^-$ with S_2 or S_3 is neglected, because it is relatively slow ($t_{1/2} \geqslant 30$ s) [15]. The back reaction rate k of Q_A^- oxidation by S_2 is 0.25 s^{-1} [15]. It should be noted that in the calculations below the exchange parameters E_1–E_4 are assumed to remain constant during the flash train.

In order to calculate the O_2 evolution as a function of flash number and exchange parameters, the relative concentration of the S-states as a function of the state at the PS II acceptor side before a flash is calculated. In this way, 32 concentrations have to be considered before each flash: ($S_n \cdot Q_A \cdot$ Inh), ($S_n \cdot Q_A \cdot Q_B$), ($S_n \cdot Q_A^- \cdot$ Inh) and ($S_n \cdot (Q_A \cdot Q_B)^-$) ($0 \leqslant n \leqslant 3$) in centers that have and do not have the fast one-electron donor to S_2 and S_3 in the reduced form. Subsequently, the effect of

a single-turnover flash is calculated using assumption (a), and from this also the O_2 evolution in that flash can be determined. Then, we correct for the fast one-electron donation to S_2 and S_3 occurring once in some centers (assumption (c)) by calculating the amount of electron donation by this donor that will occur in the time until the next flash is fired, based on the concentration of centers that are in state S_2 or S_3 and contain a reduced one-electron donor right after the flash (see below). Subsequently, from the corrected relative concentrations of the S-states as a function of the state at the acceptor side the relative concentrations of these states just before the next flash are calculated, using Eqs. 1–3. Then, the O_2 evolution at the next flash can be determined, etc. This procedure is followed for the first ten flashes after dark adaptation.

In order to simplify the calculations the states that (directly or indirectly) can neither back-react nor be formed by a back-reaction of Q_A with S_2 or S_3 (i.e., $(S_0 \cdot Q_A \cdot Q_B)$, $(S_0 \cdot (Q_A \cdot Q_B)^-)$, $(S_0 \cdot Q_A \cdot \text{Inh})$, $(S_0 \cdot Q_A^- \cdot \text{Inh})$, $(S_1 \cdot (Q_A \cdot Q_B)^-)$, $(S_1 \cdot Q_A^- \cdot \text{Inh})$, $(S_3 \cdot Q_A \cdot Q_B)$ and $(S_3 \cdot Q_A \cdot \text{Inh})$) are separated from the others. When calculating the time-dependent concentrations of the states that cannot back-react nor be formed by a back-reaction, the equations as shown in part B of the Appendix were used; for the other states, the equations from part A of the Appendix were applied.

The equations shown in the Appendix neglect the donation of one electron to S_2 or S_3 in a fraction of reaction chains by the unknown donor with $t_{1/2} = 1.4$ s (see assumption (c)). Considering this subtlety in Eqs. 4–7 would increase the mathematical effort unjustifiably, especially when we bear in mind that the donor capacity is assumed not to be restored during the measurements. Thus, the donor concentration decreases after the beginning of the flash train. Hence, we calculated the amount of S_2/S_3 reduced by the unknown donor between two flashes simply by taking the relative concentrations of S_2/S_3 and the remnants of the fast one-electron donor directly after the flash. This amount of conversion from $D \cdot S_n \cdot (Q_A \cdot Q_B/\text{Inh})^{(-)}$ to $D^+ \cdot S_{n-1} \cdot (Q_A \cdot Q_B/\text{Inh})^{(-)}$ (D is the one electron donor) was added to the amount of $(D^+) \cdot S_{n-1} \cdot (Q_A \cdot Q_B/\text{Inh})^{(-)}$ (in the corresponding state of the quinone/inhibitor complex) already present directly after the flash and subtracted from the amount of $D \cdot S_n \cdot (Q_A \cdot Q_B/\text{Inh})^{(-)}$ present at the moment directly after the first of the two flashes. These corrected concentrations are used as the concentrations at $t = 0$ after the flash.

Using these considerations and the equations shown in the Appendix, and using the Kok model [14] [including the dependence of the miss and double-hit parameters on the redox state of Q_A and on whether Q_B or Inh is bound to the quinone/inhibitor binding environment (see assumption (a))], the O_2 production in each flash can be calculated as a function of exchange parameters and flash frequency. The O_2 production in the nth flash (Y_n) can be calculated from the S-state distribution as:

$$Y_n = \beta\left([S_2 \cdot Q_A \cdot Q_B]_n + [S_2 \cdot (Q_A \cdot Q_B)^-]_n\right) + (1-\alpha)\left([S_3 \cdot Q_A \cdot Q_B]_n + [S_3 \cdot (Q_A \cdot Q_B)^-]_n + [S_3 \cdot Q_A \cdot \text{Inh}]_n\right)$$

in which $[S_2 \cdot Q_A \cdot Q_B]_n$ represents the $(S_2 \cdot Q_A \cdot Q_B)$ concentration just before the nth flash. The other concentrations are defined analogously. We have fitted theoretical values obtained from the equation to experimental values. As can be seen from reactions 1 and 2, E_1 and E_2 are dependent on the concentration of free inhibitor whereas E_3 and E_4 are not. (In principle, E_3 and E_4 are dependent on the concentration of free plastoquinone in the membrane, but since the values of E_3 and E_4 are generally found to be much smaller than about 10^3 s^{-1} expected for plastoquinone binding to the Q_B site (the $Q \rightarrow PQ$ electron transport is in the order of 1–10 ms), E_3 and E_4 are probably limited by the release of the inhibitor from the site.) Furthermore, the Q_B/inhibitor exchange is time-dependent (see Eqs. 8–15). Therefore, in order to obtain more reliable estimations of E_1–E_4, one can measure the O_2-production patterns at variable inhibitor concentration and flash frequency; in this way, many flash patterns can be obtained that have to be fitted by using four parameters. The O_2-production as a function of flash number in the first ten

flashes after dark adaptation was measured at four different flash frequencies (4, 2, 1 and 0.5 Hz) in the presence of three different concentrations (1, 2 and 4 μM) of *o*-phenanthroline or *i*-dinoseb. In this way, for one experiment 120 data points were obtained, and a unique and very reproducible solution for the values of the best-fitting exchange parameters could be obtained.

The calculated values were fitted to the experimental values by means of a least-squares fit. It was checked that the amount of inhibition at the best-fitting set of exchange parameters was in approximate agreement with the actual average inhibition of O_2-evolution in the first ten flashes. Since the absolute amplitude of the O_2-evolution is not very quantitative when using a Joliot-type O_2-electrode, a difference of approx. 20% between calculated and estimated O_2-evolution was often observed.

For *o*-phenanthroline, the best-fitting set of exchange parameters is found to be:

$E_1 = 0.32\,\mu M^{-1}\cdot s^{-1}$

$E_2 = 0.034\,\mu M^{-1}\cdot s^{-1}$

$E_3 = 0.19\,s^{-1}$

$E_4 = 0.11\,s^{-1}$

The comparison of calculated and experimental data is given in Table II. The decreasing O_2 evolution at increasing flash frequency indicates that *o*-phenanthroline is a better inhibitor at higher flash frequency. This is confirmed by measurements of the flash-induced steady-state O_2-evolution and DCIP-reduction in the presence of 1–4 μM *o*-phenanthroline (data not shown).

For *i*-dinoseb, the best fit between theory and experimental data is obtained for:

$E_1 = 0.032\,\mu M^{-1}\cdot s^{-1}$

$E_2 = 0.54\,\mu M^{-1}\cdot s^{-1}$

$E_3 = 0.009\,s^{-1}$

$E_4 = 0.18\,s^{-1}$

In Table III the experimental and calculated values are listed at three different *i*-dinoseb concentrations and four flash frequencies.

The exchange parameters observed for *o*-phenanthroline show that the affinity of *o*-phenanthroline for binding to the inhibitor/Q_B binding environment is much higher when the quinone complex is oxidized than when it is semireduced. This is in good agreement with the hypothesis of Q_B having a low and Q_B^- having a high affinity for the inhibitor/Q_B-binding environment. The approx. 10-fold difference in *o*-phenanthroline binding constant may reflect the apparent equilibrium constant of the $Q_A^- \cdot Q_B \leftrightarrows Q_A \cdot Q_B^-$ equilibrium, which is in this order of magnitude [16]. The displacement of *o*-phenanthroline by Q_B appears to be relatively insensitive to the redox state of Q_A ($E_3 \approx E_4$). This indicates that the release rate of *o*-phenanthroline is not modified greatly by reduction of Q_A because the rate-limiting step in this displacement is the release of *o*-phenanthroline (Q_B is able to bind to the binding environment in the sub-millisecond to millisecond time-scale in order to allow fast electron transport through the $Q_A \cdot Q_B$ complex). A model for *o*-phenanthroline binding is given in Fig. 2.

The binding and release kinetics of *i*-dinoseb, however, do not seem to behave like those of *o*-phenanthroline. The E_2 and E_4 values are high,

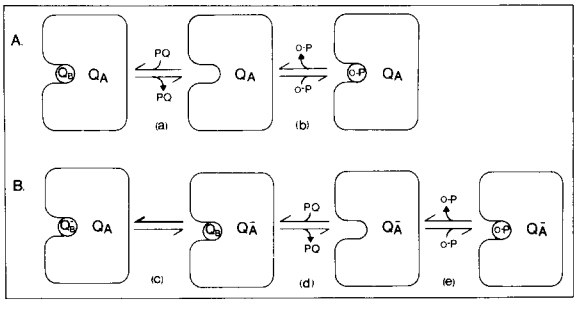

Fig. 2. A model for the interaction between *o*-phenanthroline (*o*-P) and plastoquinone (PQ) for binding to the inhibitor/Q_B-binding environment in the oxidized (A) and semireduced (B) form of the $Q_A \cdot Q_B$ or $Q_A \cdot$Inh complex. It should be stressed that the moiety creating the binding environment for $Q_A^{(-)}$, and for *o*-phenanthroline and plastoquinone may contain more than one protein. In order to minimize complexity, a real binding competition between *o*-phenanthroline and plastoquinone is suggested here. However, the inhibitor-Q_B interaction may also be allosteric [17].

and E_1 and E_3 are low, indicating that the inhibitor-quinone exchange is faster in the presence of a semiquinone than when the quinones are oxidized. Since $E_1/E_3 = E_2/E_4$, the *i*-dinoseb affinity seems to be just as large for the semiquinone complex as for the oxidized complex. Since the Q_B^- affinity is assumed to be much higher than that of Q_B, this would indicate that also the *i*-dinoseb affinity is increased upon formation of Q_A^-. However, we cannot exclude that in case of *i*-dinoseb one of the assumptions stated above is incorrect. For example, the *i*-dinoseb/Q_B interaction may not be ideally competitive, or the exchange parameters may change during the flash train. It should be stressed

TABLE II

FLASH PATTERNS IN THE PRESENCE OF *o*-PHENANTHROLINE

Experimental (E) and calculated (C) O_2 evolution by pea thylakoids in the first ten flashes after dark adaptation as a function of flash frequency in the presence of 1, 2 or 4 μM *o*-phenanthroline. All flash patterns are normalized to an average O_2 evolution of 1.0. The calculated fraction (F) of O_2 evolution in the first ten flashes in the presence of *o*-phenanthroline as compared to the control is also indicated in the table. The control values for α and β were 0.13 and 0.04, respectively.

Flash frequency (Hz)		0.5		1		2		4	
[*o*-Phenanthroline] (μM)	Flash number	E	C	E	C	E	C	E	C
1	1	0	0	0	0	0	0	0	0
	2	0.11	0.20	0.18	0.24	0.19	0.27	0.21	0.29
	3	2.00	1.94	2.24	2.17	2.48	2.43	2.79	2.64
	4	1.56	1.48	1.43	1.40	1.35	1.32	1.15	1.25
	5	1.03	1.03	0.85	0.84	0.72	0.67	0.57	0.54
	6	0.85	0.91	0.77	0.80	0.69	0.70	0.65	0.64
	7	1.13	1.13	1.29	1.23	1.47	1.36	1.66	1.49
	8	1.18	1.17	1.26	1.24	1.29	1.31	1.30	1.36
	9	1.11	1.10	1.03	1.07	0.95	1.02	0.86	0.94
	10	1.02	1.05	0.95	1.00	0.86	0.93	0.81	0.86
	F		0.54		0.48		0.44		0.41
2	1	0	0	0	0	0	0	0	0
	2	0.09	0.17	0.13	0.21	0.19	0.24	0.25	0.27
	3	1.76	1.75	1.94	1.98	2.21	2.26	2.48	2.50
	4	1.51	1.49	1.44	1.42	1.36	1.35	1.21	1.27
	5	1.19	1.20	1.07	1.02	0.89	0.82	0.71	0.64
	6	1.01	1.06	0.96	0.95	0.86	0.81	0.75	0.71
	7	1.09	1.09	1.17	1.14	1.28	1.24	1.45	1.39
	8	1.12	1.10	1.17	1.15	1.23	1.22	1.27	1.30
	9	1.11	1.08	1.10	1.09	1.02	1.06	0.98	0.99
	10	1.12	1.06	1.04	1.05	0.96	1.00	0.90	0.93
	F		0.43		0.36		0.31		0.27
4	1	0	0	0	0	0	0	0	0
	2	0.08	0.14	0.10	0.17	0.16	0.21	0.20	0.24
	3	1.55	1.55	1.70	1.76	2.00	2.03	2.37	2.30
	4	1.47	1.48	1.47	1.45	1.40	1.40	1.28	1.32
	5	1.29	1.30	1.22	1.19	1.03	1.01	0.87	0.80
	6	1.12	1.18	1.08	1.10	0.96	0.96	0.78	0.82
	7	1.10	1.13	1.09	1.11	1.17	1.14	1.32	1.26
	8	1.12	1.09	1.12	1.10	1.15	1.14	1.20	1.21
	9	1.15	1.07	1.11	1.08	1.10	1.07	1.00	1.04
	10	1.11	1.06	1.11	1.05	1.03	1.04	0.97	1.00
	F		0.34		0.27		0.22		0.18

that the minimum of O_2-evolution always observed at the fourth flash in the presence of rather high concentrations of *i*-dinoseb at long flash intervals (Table III) cannot be accounted for by the model used. Furthermore, *i*-dinoseb may have additional effects at the donor side of Photosystem II (K. Pfister, personal communication). Another reason for discrepancies found may be that the model is too much simplified; for example, it does not include 'non-B-type centers' [18], i.e., centers which are hypothesized not be able to bind Q_B, and that have to transfer electrons to another electron acceptor.

It should be stressed that every combination of exchange parameters yields its unique set of predicted O_2 yields at different flash frequencies and

TABLE III

FLASH PATTERNS IN THE PRESENCE OF *i*-DINOSEB

Experimental (E) and calculated (C) O_2 evolution by pea thylakoids in the first ten flashes after dark adaptation as a function of flash frequency in the presence of 1, 2 or 4 μM *i*-dinoseb. The control values of α and β were 0.13 and 0.04, respectively. The flash patterns are normalized to an average O_2 evolution of 1.0. The calculated fraction F of O_2 evolution in the first ten flashes in the presence of *i*-dinoseb as compared to the control is indicated at the bottom line at each inhibitor concentration.

Flash frequency (Hz)		0.5		1		2		4	
[*i*-Dinoseb] (μM)	Flash number	E	C	E	C	E	C	E	C
1	1	0	0	0	0	0	0	0	0
	2	0.10	0.18	0.14	0.19	0.23	0.22	0.26	0.24
	3	1.47	1.48	1.57	1.67	1.83	1.91	2.17	2.18
	4	1.39	1.37	1.36	1.32	1.27	1.25	1.17	1.19
	5	1.23	1.21	1.09	1.05	0.90	0.86	0.72	0.69
	6	1.13	1.14	1.00	1.01	0.87	0.88	0.74	0.77
	7	1.15	1.16	1.22	1.20	1.32	1.29	1.46	1.41
	8	1.19	1.17	1.23	1.23	1.32	1.30	1.37	1.36
	9	1.16	1.15	1.21	1.18	1.15	1.17	1.06	1.11
	10	1.19	1.14	1.18	1.15	1.11	1.14	1.05	1.07
	F		0.30		0.32		0.34		0.33
2	1	0	0	0	0	0	0	0	0
	2	0.08	0.16	0.16	0.16	0.19	0.18	0.35	0.21
	3	1.32	1.28	1.39	1.44	1.66	1.63	1.95	1.88
	4	1.30	1.34	1.33	1.34	1.27	1.27	1.24	1.20
	5	1.30	1.28	1.19	1.21	1.03	1.04	0.86	0.85
	6	1.23	1.24	1.17	1.16	0.97	1.04	0.85	0.90
	7	1.19	1.21	1.16	1.19	1.23	1.22	1.31	1.31
	8	1.20	1.19	1.23	1.19	1.28	1.24	1.31	1.31
	9	1.19	1.17	1.19	1.17	1.17	1.20	1.09	1.19
	10	1.20	1.15	1.19	1.15	1.19	1.18	1.05	1.17
	F		0.20		0.22		0.22		0.19
4	1	0	0	0	0	0	0	0	0
	2	0.11	0.15	0.16	0.14	0.30	0.16	0.36	0.17
	3	1.21	1.15	1.26	1.26	1.45	1.40	1.75	1.58
	4	1.11	1.29	1.22	1.34	1.24	1.32	1.22	1.23
	5	1.26	1.28	1.22	1.29	1.16	1.21	1.06	1.04
	6	1.29	1.26	1.23	1.24	1.14	1.18	0.99	1.05
	7	1.26	1.24	1.22	1.22	1.16	1.21	1.18	1.24
	8	1.24	1.22	1.22	1.19	1.21	1.20	1.27	1.26
	9	1.25	1.21	1.28	1.17	1.20	1.18	1.09	1.22
	10	1.28	1.19	1.20	1.15	1.14	1.16	1.08	1.21
	F		0.11		0.13		0.13		0.13

inhibitor concentrations. The method used here is able to measure straightforwardly whether an inhibitor exchanges with Q_B on a time scale of 0.1–10 s. Unfortunately, the quantitative determination of the exchange parameters is somewhat elaborate with this method, but with the help of a computer the calculations can be done very quickly.

Acknowledgements

This research was supported by the Deutsche Forschungsgemeinschaft. W.V. acknowledges financial support by the Deutsche Akademische Austauschdienst. We thank Dr. C. Kötter (Schering AG, Berlin) and Dr. W. Oettmeier (Ruhr Universität, Bochum) for the kind gifts of pea seeds and *i*-dinoseb, respectively.

Appendix

Equations for the calculation of the concentration of Photosystem-II centers in a certain state of the water-splitting system and the quinone complex as a function of exchange parameters and time

(A) In case a back-reaction of Q_A with the S-states can occur

If a back-reaction can occur, the concentration changes of the different states using the above-stated assumptions can be calculated from Eqns. 4–7:

$$d[S_n \cdot Q_A^- \cdot Inh]/dt = E_2[S_n \cdot (Q_A \cdot Q_B)^-]_t - (k + E_4)[S_n \cdot Q_A^- \cdot Inh]_t \quad (4)$$

$$d[S_n \cdot (Q_A \cdot Q_B)^-]/dt = E_4[S_n \cdot Q_A^- \cdot Inh]_t - E_2[S_n \cdot (Q_A \cdot Q_B)^-]_t \quad (5)$$

$$d[S_n \cdot Q_A \cdot Inh]/dt = k[S_{n+1} \cdot Q_A^- \cdot Inh]_t + E_1[S_n \cdot Q_A \cdot Q_B]_t - E_3[S_n \cdot Q_A \cdot Inh]_t \quad (6)$$

$$d[S_n \cdot Q_A \cdot Q_B]/dt = E_3[S_n \cdot Q_A \cdot Inh] - E_1[S_n \cdot Q_A \cdot Q_B]_t \quad (7)$$

The solution for Eqn. 4 is:

$$[S_n \cdot Q_A^- \cdot Inh]_t = A_1 e^{-\lambda_1 t} + A_2 e^{-\lambda_2 t} \quad (8)$$

where

$$\lambda_1 = \tfrac{1}{2}\left\{E_2 + E_4 + k + \sqrt{(E_2 + E_4 + k)^2 - 4E_2 k}\right\}$$

$$\lambda_2 = \tfrac{1}{2}\left\{E_2 + E_4 + k - \sqrt{(E_2 + E_4 + k)^2 - 4E_2 k}\right\}$$

$$A_1 = \left\{(\lambda_2 - E_4 - k)[S_n \cdot Q_A^- \cdot Inh]_0 + E_2[S_n \cdot (Q_A \cdot Q_B)^-]_0\right\}/(\lambda_2 - \lambda_1)$$

$$A_2 = [S_n \cdot Q_A^- \cdot Inh]_0 - A_1$$

From Eqn. 5:

$$[S_n \cdot (Q_A \cdot Q_B)^-]_t = B_1 \cdot e^{-E_2 t} + \frac{E_4 A_1}{E_2 - \lambda_1} e^{-\lambda_1 t} + \frac{E_4 A_2}{E_2 - \lambda_2} e^{-\lambda_2 t} \quad (9)$$

where:

$$B_1 = [S_n \cdot (Q_A \cdot Q_B)^-]_0 - \frac{E_4 A_1}{E_2 - \lambda_1} - \frac{E_4 A_2}{E_2 - \lambda_2}$$

From Eqn. 6:

$$[S_n \cdot Q_A \cdot Inh]_t = C_1 \cdot e^{-(E_1 + E_3)t} + C_2 + \mu_1 e^{-\lambda_1 t} + \mu_2 e^{-\lambda_2 t} \quad (10)$$

where:

$$\mu_1 = \frac{E_1 k A_1 - k\lambda_1 A_1}{\lambda_1^2 - E_1\lambda_1 - E_3\lambda_1}$$

$$\mu_2 = \frac{E_1 k A_2 - k\lambda_2 A_2}{\lambda_2^2 - E_1\lambda_2 - E_3\lambda_2}$$

$$C_1 = (E_3[S_n \cdot Q_A \cdot Inh]_0 - k[S_{n+1} \cdot Q_A^- \cdot Inh]_0 - E_1[S_n \cdot Q_A \cdot Q_B]_0 - \mu_1\lambda_1 - \mu_2\lambda_2)/(E_1 + E_3)$$

$$C_2 = [S_n \cdot Q_A \cdot Inh]_0 - C_1 - \mu_1 - \mu_2$$

From Eqn. 7:

$$[S_n \cdot Q_A \cdot Q_B]_t = D_1 e^{-E_1 t} - C_1 e^{-(E_1 + E_3)t} + \frac{E_3}{E_1} C_2 + \frac{E_3 \mu_1}{E_1 - \lambda_1} e^{-\lambda_1 t} + \frac{E_3 \mu_2}{E_1 - \lambda_2} e^{-\lambda_2 t} \quad (11)$$

where:

$$D_1 = [S_n \cdot Q_A \cdot Q_B]_0 + C_1 - \frac{E_3}{E_1} C_2 - \frac{E_3 \mu_1}{E_1 - \lambda_1} - \frac{E_3 \mu_2}{E_1 - \lambda_2}$$

(B) In case the Q_A^- oxidation by the S-states cannot occur ($k = 0$)

If the Q_A^- oxidation cannot occur ($k = 0$), the differential equations 4–7 can be solved by standard differential equation calculus:

$$[S_n \cdot Q_A^- \cdot Inh]_t = E_2\sigma_2 + ([S_n \cdot Q_A^- \cdot Inh]_0 - E_2\sigma_2)e^{-(E_2+E_4)t} \quad (12)$$

$$[S_n \cdot (Q_A \cdot Q_B)^-]_t = E_4\sigma_2 + ([S_n \cdot (Q_A \cdot Q_B)^-]_0 - E_4\sigma_2)e^{-(E_2+E_4)t} \quad (13)$$

$$[S_n \cdot Q_A \cdot Inh]_t = E_1\sigma_1 + ([S_n \cdot Q_A \cdot Inh]_0 - E_1\sigma_1)e^{-(E_1+E_3)t} \quad (14)$$

$$[S_n \cdot Q_A \cdot Q_B]_t = E_3\sigma_1 + ([S_n \cdot Q_A \cdot Q_B]_0 - E_3\sigma_1)e^{-(E_1+E_3)t} \quad (15)$$

in which:

$$\sigma_1 = ([S_n \cdot Q_A \cdot Q_B]_0 + [S_n \cdot Q_A \cdot Inh]_0)/(E_1 + E_3)$$

$$\sigma_2 = ([S_n \cdot (Q_A \cdot Q_B)^-]_0 + [S_n \cdot Q_A^- \cdot Inh]_0)/(E_2 + E_4)$$

As expected, the same results can be obtained from Eqn. 8–11 by substituting $k = 0$.

References

1 Fedtke, C. (1982) Biochemistry and Physiology of Herbicide Action, Springer-Verlag, Berlin
2 Van Rensen, J.J.S. (1982) Physiol. Plant. 54, 515–521
3 Vermaas, W.F.J., Arntzen, C.J., Gu, L.-Q. and Yu, C.-A. (1983) Biochim. Biophys. Acta 723, 266–275
4 Wraight, C.A. (1981) Isr. J. Chem. 21, 348–354
5 Velthuys, B. (1981) FEBS Lett. 126, 277–281
6 Tischer, W. and Strotmann, H. (1977) Biochim. Biophys. Acta 460, 113–125
7 Laasch, H., Pfister, K. and Urbach, W. (1982) Z. Naturforsch. 37c, 620–631
8 Vermaas, W.F.J. and Arntzen, C.J. (1983) Biochim. Biophys. Acta 725, 483–491
9 Lavergne, J. (1982) Biochim. Biophys. Acta 682, 345–353
10 Taoka, S., Robinson, H.H. and Crofts, A.R. (1983) in The Oxygen Evolving System of Plant Photosynthesis (Inoue, Y., Crofts, A.R., Govindjee, Murata, N., Renger, G. and Satoh, K., eds.), pp. 360–382, Academic Press, Tokyo
11 Wraight, C.A. and Stein, R.R. (1980) FEBS Lett. 113, 73–77
12 Laasch, H., Schreiber, U. and Urbach, W. (1983) FEBS Lett. 159, 275–279
13 Joliot, P., Barbieri, G. and Chabaud, R. (1969) Photochem. Photobiol. 10, 309–329
14 Kok, B., Forbush, B. and McGloin, M. (1970) Photochem. Photobiol. 11, 457–475
15 Vermaas, W.F.J., Renger, G. and Dohnt, G. (1984) Biochim. Biophys. Acta 764, 194–202
16 Robinson, H.H. and Crofts, A.R. (1983) FEBS Lett. 153, 221–226
17 Vermaas, W.F.J., Renger, G. and Arntzen, C.J. (1984) Z. Naturforsch., in the press
18 Lavergne, J. (1982) Photobiochem. Photobiophys. 3, 257–271